7th ECCOMAS Thematic Conference on Smart Structures and Materials
SMART 2015
A.L. Araújo, C.A. Mota Soares, et al. (Editors)

STRUCTURAL DAMAGE QUANTIFICATION BASED ON RECURRENCE PLOTS AND RELAXATION METHOD OF PARTICLE FILTER

Yasutoshi Nomura[*] , Tadanobu SATO[†], Hitoshi FURUTA[†]

[*]Ritsumeikan University
1-1-1 Noji-Higashi, Kusatsu, 525-8577 Japan
y-nomura@fc.ritsumei.ac.jp

[†]Southeast University
2 Sipailou Street, Nanjing 210096, Jiangsu, China
satotdnb@yahoo.co.jp

[†]Kansai University
2-1-1 Ryozenji-cho, Takatsuki, 569-1095, JAPAN
furuta@res.kutc.kansai-u.ac.jp

Key words: Structural damage quantification, recurrence plots, particle filter.

Summary: *In this paper, chaotic excitation is proposed to vibrate the structures. The attractors reconstructed from the structural responses are used for the early-stage damage detection. After the damage is detected, it is further quantified using the Particle Filter technique. Laboratory experiment using a 4-story building subjected to chaotic excitation is carried out. The experimental results demonstrated that the proposed approach will be helpful for detecting and quantifying damage levels at the early stage for the structural health monitoring.*

1 INTRODUCTION

The structural health monitoring of civil engineering structures is a fundamental issue for structural safety and integrity, due to the fact that they will deteriorate just after they are built and put into services. The failure of structures will not only result in severe economic lost but may threaten the lives of people. Hence maintaining safety and reliable civil engineering structures for daily use is an extremely important issue which has received considerable attention in literature in recent years. Deterioration of the structure often refers to the structural damage and it can be reflected by the "deterioration" of the structural parameters. In practice, damage was defined as the changes introduced into a system which adversely affected its current or future performance. Therefore changes in structural parameters have been extensively applied as effective tools for damage detection. An overview of some modal-based approaches can be found in literatures [1, 2, 3]. However, it is difficult to detect the location of damage to structure because the change of those modal features due to damage is minor. Besides modal-based methods, auto-regressive approach [4, 5], neural networks [6], wavelet analysis have been proposed and successfully applied to various fields for this purpose [7, 8,

9]. Among which, the vibration-based damage identification (VBDI) methods draws extensive attention and are deeply developed.

Meahwhile, the deterioration of the civil engineering structures usually begins from the local and small damages. Small damages gradually develop and become large damages and at last cause failure of the structure. For the consideration of the structural safety and reliability, detecting small damages is essential and useful. Therefore, to detect minor damages, development of other approaches is necessary, in which chaos attractor-based analysis [10, 11, 12, 13] seems to be a promising way. The recent study has demonstrated that the damage-induced change of the attractor is larger than that of the most sensitive frequency of the vibrational response of the structure [12]. It should be noted that past researches on attractor-based approach can successfully identify the damage existence, and some of them can also quantify the damage, but damage localization has not been discussed sufficiently although localizing damage is very important in SHM.

A first attempt in this paper is made to explore an attractor-based health monitoring system using chaotic excitation for the purpose of the damage localization. In evaluation of reconstructed attractor, the recurrence plot is applied to detect damage-induced change. The recurrence plots [14] were designed to detect non-stationarity in time series data and can be therefore a candidate for detecting damage location from structural response data. However, detection alone may not be sufficient for the purpose of damage evaluation and structural maintenance. In this case, damage requires to be further quantified.

The second attempt is made to explore merging particle filter (MPF) for damage quantification by identifying structural parameters. The MPF is an improved algorithm of the particle filter (PF), in which filtering is performed by merging several particles of a prior ensemble, which is rather similar to the genetic algorithm [15]. Thus the structural deterioration can be detected and evaluated at the early stage and proper relevant measurement can be applied to ensure the safety of the structures.

2 DAMAGE LOCALIZATION BY RECURRENCE PLOTS

2.1 Recurrence plots

The recurrence plot is a graphical technique designed to highlight structure (i.e. determinism) in signals. It might be thought of as a global, probabilistic autocorrelation function that considers the relative frequencies at which a system returns to a given dynamical state. Presuming a dynamical system governed by $\dot{\mathbf{x}}=F(\mathbf{x})$, then based on the response observed at T discrete points in time ($\mathbf{x}(i)$, $i=1,2,\ldots,T$) the threshold recurrence plot is formally constructed by forming the matrix

$$R_{i,j} = \Theta(\varepsilon - \|\mathbf{x}(i) - \mathbf{x}(j)\|), \tag{1}$$

where ε is a threshold value representing the specific length scale of focus and $\|\mathbf{x}(i)-\mathbf{x}(j)\|$ takes the Euclidean distance of the m-dimensional vector. Using the Heaviside function Θ, the values of Ri,j are 1 or 0, respectively depending on whether the distance between points $\mathbf{x}(i)$ and $\mathbf{x}(j)$ is less than or greater than a threshold value ε. A plot of the recurrence matrix is designated as the recurrence plot. For a single observed variable $\mathbf{x}(i)$ the familiar delay coordinate approach can also be used. Delay coordinate reconstruction is the standard first step in most non-linear time series analysis and proceeds by forming the reconstructed dynamics

$$\mathbf{x}(n) = \big(x(n), x(n+T), \ldots, x(n+(m-1)T)\big) \tag{2}$$

with delay T and embedding dimension m.

Recurrence plots were designed to detect non-stationarity in time series data. They are therefore candidates for detecting damage-induced change in structural response data. In previous applications, analysis of recurrence plots has demonstrated superior performance to linear-based approaches in time series data [16]. In this study, features to detect damage-induced change of structural response are extracted from the recurrence matrix $R_{i,j}$.

2.2 Percent recurrence

Percent recurrence is simply the percentage of darkened points. For a T point time series, this measure is given simply as

$$\%recurrence = \frac{\sum_{i=1}^{T}\sum_{j=1}^{T} R_{i,j}}{T^2}. \tag{3}$$

This particular metric reflects the frequency that a given trajectory will visit a local region of phase space defined by ε. Figure 1 presents examples of recurrence plots for outputs of Lorenz system and a Gaussian noise.

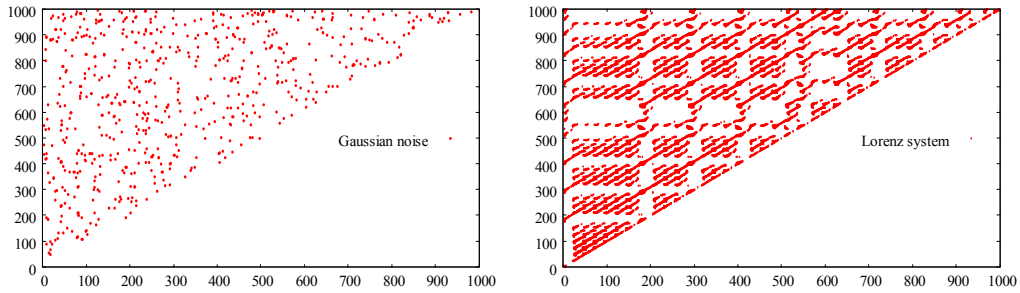

(a) Recurrence plots of Gaussian noise (b) Recurrence plots of Lorenz system

Figure 1. Examples of Recurrence plots.

As shown in Fig. 1(a), from recurrence points of Gaussian noise, no kind of deterministic structure can be seen because near points at time i are not near at time i+1. However, the diagonal line structures are apparent in the results of recurrence plots for Lorenz system, as depicted in Fig. 1(b). The diagonal lines are representative of deterministic dynamics. The chaotic processes typically exhibit usually short diagonal structures of length related to the inverse of the positive Lyapunov exponent because the Lyapunov exponents evaluate the local exponential divergence or convergence of nearby trajectories. Trajectories remain near for a short time before diverging because of the sensitive dependence on initial conditions.

2.3 Damage localization by percent recurrence

In attractor-based approach using chaotic input is extremely important to excite the structure in a way that the dimension of the response is sufficiently low to allow robust detection of feature which quantifies the damage. As pointed in reports of recent studies [10, 11, 12], chaotic excitation must be tuned properly according to the structure's Lyapunov exponent spectrum, which is expressed with the modal damping rate observed from eigenvalues. However, in the case in which a structure which has a very low damping ratio at each mode is monitored with this approach, a chaotic signal with very low-frequency band must be tuned and is input into the structure. In such case, it is considered that the amplitude of vibration of

the structure become very low, which causes some difficulties on evaluation of response data. The procedure of damage localization is presented in Table 1.

Step 1	Input Chaotic signal to Structure and Observe relative story acceleration
Step 2	Extraction of the first mode vibration at all measurement points
Step 3	Reconstruction of Attractor
Step 4	Observation of Baseline data (a) Calculation of %recurrence (%*REC*) using Threshold value ε_{own} and $\varepsilon_{i\text{th}}$ ε_{own}: 10% of standard deviation of wavelet coefficients at the own sensor. $\varepsilon_{i\text{th}}$: 10% of standard deviation of wavelet coefficients at the sensor *i* $\%REC_{\text{own}}(s)$, $\%REC_{1\text{st}}(s)$, $\%REC_{i\text{th}}(s)$, are observed. (*i*, *s*: sensor number) (b) Normalization of %REC $NREC_{1\text{st}}(s) = \%REC_{\text{own}}(s) / \%REC_{1\text{st}}(s)$ $NREC_{2\text{nd}}(s) = \%REC_{\text{own}}(s) / \%REC_{2\text{nd}}(s)$ $NREC_{i\text{th}}(s) = \%REC_{\text{own}}(s) / \%REC_{i\text{th}}(s)$ …
Step 5	Input Chaotic signal used in Step 1 to the damaged structure and Steps 2–4 are performed.
Step 6	Calculation of Damage Index $\mathrm{DI}(s) = \max\left[\frac{NREC_{1\text{st}}^{\text{damage}}(s)}{NREC_{1\text{st}}^{\text{Intact}}(s)}, \ldots, \frac{NREC_{4\text{th}}^{\text{damage}}(s)}{NREC_{4\text{th}}^{\text{Intact}}(s)}\right]$ DI(s) = 1.0: Intact DI(s) ≠ 1.0: Damage

Table 1. Procedure of damage localization.

In the first step (Step 1) of this study, a normal chaotic signal, which is not tuned properly, is input into the structure and relative story acceleration is measured at each sensor. When an untuned chaotic signal is input into the structure, high dimensional response with several vibration modes is regarded as excited. Results of our past studies confirmed that damage location cannot be detected precisely by merely evaluating an attractor reconstructed from response with several vibration modes. In this study, we attempt to extract the first mode vibration from the response data in Step 2 and to evaluate the reconstructed attractor from the first mode vibration in Step 3. The first mode impulse vibration can be detected easily using experimental modal analysis. However, parameters of some kinds such as initial values of modal damping, and the weight matrix might vary the results. Using the proposed method, wavelet coefficients corresponding to the first mode vibration are extracted by application of continuous wavelet transform.

In the Step 4, baseline data are acquired by calculating several *%REC*s from reconstructed attractor and normalizing them. Usually, the result of *%REC* is dependent on the threshold values, ε, in Eq. (1). $\%REC_{\text{own}}(s)$ in Table 1 is the result of auto percent recurrence observed at the sensor s, in which 10% value of the standard deviation of wavelet coefficients calculated from own response at the sensor *s* is set as threshold value, ε_{own}. In other words, $\%REC_{\text{own}}(s)$ is the result obtained using one's own statistical information as the threshold value, ε_{own}. Meanwhile, $\%REC_{i\text{th}}(s)$ is also the result of auto percent recurrence observed at the sensor *s*.

At this time, threshold value $\varepsilon_{i\text{th}}$ is calculated from the standard deviation of wavelet coefficients observed from the sensor *i*. In short, $\%REC_{i\text{th}}(s)$ is calculated at the sensor *s* using statistical information observed at different sensor.

In this study, *%REC* is calculated individually in each intact situation and damage situation without calculating cross-percent recurrence, and the normalized value, $NREC_{i\text{th}}$ ($=\%REC_{\text{own}} / \%REC_{i\text{th}}$), is compared before and after damage to detect the location of damage to the structure. $NREC_{i\text{th}}$ denotes the relative relation of $\%REC_{\text{own}}$ at each measurement point in intact and damage situations. If the dynamics of the test attractor are altered because of damage, then it is clear that the relative relation of $\%REC_{\text{own}}$ will be altered according to the change.

In step 6, the *Damage Index* (*DI*), which is expressed as a maximum value of $NREC_{i\text{th}}^{\text{damage}}/NREC_{i\text{th}}^{\text{intact}}$ is evaluated to detect the damage location to the structure. If $DI(s)$ is shown to be about 1.0, then it can be considered that the structural condition at the story with sensor *s* remains unchanged after damages and is intact. However, if DI(s) ≠ 1, then it can be considered that the structural condition of the story with sensor *s* has some abnormality or that it is damage. Through these steps, the proposed method can extract a difference between damaged location and intact location.

3 DAMAGE QUANTIFICATION BY RELAXATION METHOD OF PERTICLE FILTER

3.1 Particle filter

Particle filter technique (PF) is one of recursive filtering techniques composed of the prediction and observation updating processes [17, 18].
The general state space model is described by the state transfer and observation equations as follows:

$$\begin{aligned} x_t &= F(x_{t-1}, w_{t-1}) \\ y_t &= H(x_t, v_t) \end{aligned} \tag{4}$$

in which, t is the discrete time step, x_t the state vector, y_t the observation vector, w_t the system noise vector and v_t the observation noise vector which is assumed to be expressed by

$$v_t = H^{-1}(y_t, x_t) = G(y_t, x_t). \tag{5}$$

The particle filter (PF) can be applied even if the state space model is non-linear and non-Gaussian. In the PF, the probability density function of the state vector is expressed by many realizations, called particles and of which time marching behavior is calculated step by step. The PF is therefore an algorithm to identify particles which express the conditional probability density function $p(x_t|Y_t)$ instead of identifying the state vector x_n directly. $Y_t=\{y_t, y_{t-1}, \cdots, y_1\}$ is the assemble of observation vectors. We called $p(x_t|Y_{t-1})$ as the prediction distribution and $p(x_t|Y_t)$ as the filter distribution, and each probability density function (PDF) is approximated by n realizations as follows:

$$x_{t-1|t-1}^{(j)} \sim p(x_{t-1}|Y_{t-1}) \quad j = 1,2,\cdots,n \tag{6}$$

Cumulative distribution of x_{t-1}can be approximated by

$$P(x_{t-1}|Y_{t-1}) = \frac{1}{n}\sum_{j=1}^{n} U\left(x_{t-1} - x_{t-1|t-1}^{(j)}\right) \tag{7}$$

where U is the step function. The approximated PDF of the state vector at $(t-1)$th time step is given by the derivation of cumulative distribution function with respect to x_{t-1},

$$p(x_{t-1}|Y_{t-1}) = \frac{1}{n}\sum_{j=1}^{n} \delta\left(x_{t-1} - x_{t-1|t-1}^{(j)}\right), \tag{8}$$

where δ is the Dirac delta function. The particles of tth step before observation updating are obtained by simply substituting $(t-1)$th time step particlees into the state transfer equation,

$$x_{t|t-1}^{(j)} = F\left(x_{t-1|t-1}^{(j)}, w_{t-1}^{(j)}\right). \tag{9}$$

The approximated PDF of the state vector before updating at tth time step is estimated by particle realizations

$$p(x_t|Y_{t-1}) = \frac{1}{n}\sum_{j=1}^{n} \delta\left(x_t - x_{t|t-1}^{(j)}\right) \tag{10}$$

The PDF of the state vector after updated by adding observation data y_t is obtained through Bayesian theorem

$$p(x_t|Y_t) = p(x_t|y_t, Y_{t-1}) = \frac{p(x_t, y_t|Y_{t-1})}{p(y_t|Y_{t-1})} = \frac{p(y_t|x_t, Y_{t-1})p(x_t|Y_{t-1})}{\int p(y_t|x_t, Y_{t-1})p(x_t|Y_{t-1})dx_t} \tag{11}$$

Substituting Eq.(11) into Eq.(12) we have

$$p(x_t|Y_t) = \frac{p(y_t|x_t, Y_{t-1})\frac{1}{n}\sum_{j=1}^{n} \delta\left(x_t - x_{t|t-1}^{(j)}\right)}{\int p(y_t|x_t, Y_{t-1})\frac{1}{n}\sum_{j=1}^{n} \delta\left(x_t - x_{t|t-1}^{(j)}\right)\, dx_t} \tag{12}$$

Integration appearing in the denominator can be performed and we obtain

$$p(x_t|Y_t) = \sum_{j=1}^{n} \frac{q_t^{(j)}}{\sum_{i=1}^{n} q_t^{(i)}} \delta\left(x_t - x_{t|t-1}^{(j)}\right) = \sum_{J=1}^{n} \alpha_t^{(j)}\, \delta\left(x_t - x_{t|t-1}^{(j)}\right) \tag{13}$$

where

$$q_t^{(i)} = p\left(y_t|x_{t|t-1}^{(i)}\right) \tag{14}$$

$$\alpha_t^{(i)} = \left(\frac{q_t^{(i)}}{\sum_{j=1}^{n} q_t^{(j)}}\right). \tag{15}$$

$q_t^{(i)}$ is the likelihood of $x_{t|t-1}^{(i)}$ after the observation data y_t is given.

3.2 Relaxation method of particle filter

A significant problem with the basic particle filter algorithm is degeneration. To overcome this problem, the merging particle filter (MPF) is used in this study, as a relaxation method of particle filter. In MPF, each member of a filtered ensemble is generated from a weighted sum of multiple samples (n_m) from the predicted ensembles (n) such that the mean and covariance of the filtered distribution are approximately preserved. When the number of particles to be merged is assumed to be n_m, we draw $n_m \times n$ samples from the prediction particles with the

weight of likelihood. The algorithm of MPF is defined by the following steps, as shown in Table 2.

Step 1	Generate n initial particles $x_{0\|0}^{(j)}$ (j=1, 2, …, n) .
Step 2	Set t = 1 and repeat the following steps until the end of time step. (a) Calculate the prediction particles according to the Time updating process, $x_{t\|t\text{-}1}^{(j)} = F(x_{t\text{-}1\|t\text{-}1}^{(j)}, w_{t\text{-}1}^{(j)})$. (b) Calculate the likelihood, $q_t^{(j)} = p\left(y_t \| x_{t\|t-1}^{(j)}\right)$ (c) Obtain an ensemble $\{\hat{x}_{t\|t}^{(1,1)}, \dots, \hat{x}_{t\|t}^{(n_m,1)}, \dots, \hat{x}_{t\|t}^{(1,n)}, \dots, \hat{x}_{t\|t}^{(n_m,n)}\}$, according to $q_t^{(j)}/\sum_{m=1}^{n}\{q_t^{(m)}\}$. (d) Generate new particles $x_{t\|t}^{(j)}$ as a weighted sum of n_m samples. $x_{t\|t}^{(j)} = \sum_{k=1}^{n_m} \beta_k \hat{x}_{t\|t}^{(k,j)}$

Table 2. Procedure of merging particle filter

In order to ensure that the newly generated ensemble preserves the mean and covariance of the filtered PDF for $n\rightarrow\infty$, the merging weights β_k are set to satisfy following equations.

$$\sum_{k=1}^{n_m} \beta_k = 1, \sum_{k=1}^{n_m} \beta_k^2 = 1 \tag{16}$$

In this study, the particle (state vector) x is composed of the motions of all the nodes and unknown parameters;

$$x = (x_a\ x_b)' \qquad x_a = (\ddot{\mathbf{u}}\ \dot{\mathbf{u}}\ \mathbf{u})' \tag{17}$$

where x_b represents unknown parameters. In this study, the case in which the mass, stiffness and damping ratio at the 1st and 2nd modes of the structure are all unknown s investigated. The state equation is given by

$$x_{a,t} = F(x_{a,t\text{-}1}, x_{b,t\text{-}1}) + w_{a,t},\ x_{b,t} = x_{b,t\text{-}1} + w_{b,t}. \tag{18}$$

The $F(x)$ is the function that represents one-step prediction of structural vibration. Through comparisons between actual response acceleration and predicted one, likelihood of each particle is calculated. However, newly generated ensembles have the potential to not satisfy exactly the equation of motion because the information of response (motions of all the nodes) are generated from the weighted sum as well. Moreover, it was found in this study that all but one particle may have negligible weights while repeating update process of new ensemble even by using MPF. In this study, we examine a suitable time step to generate new ensemble instead of updating ensemble at all the time step.

4 LABORATORY EXPERIMENTS

To demonstrate the efficiency of the proposed method, laboratory experiments are conducted. Figure 2 shows the structural model. The S1, S2, …, S8 of this figure are the

accelerometers. The columns of C1 is removed or replaced with other column element to introduce damage situations. In intact situation, all columns have the width of 40 mm. Observation of acceleration is conducted for 45s at sampled at 100 Hz. Chaotic excitation in this study is given as the first state vector z_1 of the chaotic Lorenz oscillator.

$$\begin{aligned} \eta^{-1}\frac{dz_1}{dt} &= -\alpha(z_1 - z_2) \\ \eta^{-1}\frac{dz_2}{dt} &= \beta z_1 - z_2 - z_1 z_3 \\ \eta^{-1}\frac{dz_3}{dt} &= z_1 z_2 - \gamma z_3, \end{aligned} \tag{19}$$

In those equations, α=16, β=40, γ=4, and η are parameters to speed up or slow the oscillation. The initial conditions of z_1, z_2, and z_3 are set respectively to 1.0, 1.0 and 1.0. Through an exciter located at the top story chaotic signal is given to the structure.

Figure 3 shows the time history and Fourier amplitude of the signal input to the structure. The excitation exhibits a linear decay in Fourier amplitude with frequency, a characteristic of the Lorenz oscillator.

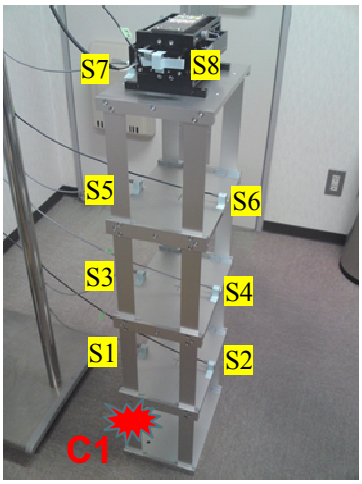

Figure 2. Structural model and exciter.

Scenario 1	Replace column C1 with a column having the width of 30mm
Scenario 2	Remove column C1

Table 3. Damage scenario.

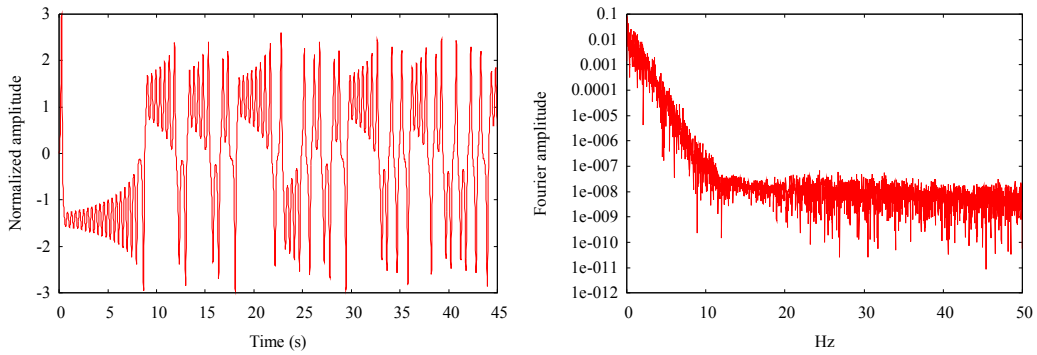

(a) Time history of chaotic excitation. (b) Fourier amplitude of chaotic excitation.

Figure 3. Time history and Fourier amplitude of input signal.

Damage scenarios described in Table 3 are used. When a 40mm-wide column is replaced with a 30mm-wide column, a 6.25% reduction in inter-story stiffness occurs at the story. In this case, the change of modal parameter before and after damage is very minor. In damage scenario 1, the change of the first mode frequency is about 1.8%. The most sensitive frequency change was found to be about 2.1% (intact 4.761 Hz, damaged 4.663 Hz) at the second mode from the response acceleration. In this case, it is difficult for modal-based methods to localize the damage because of the small change. On the other hand, when a column is removed, a 25% reduction in inter-story stiffness occurs at the story.

Regarding the attractor reconstruction, an embedded dimension of m = 3 is used for this study. A time delay of L = 1 was determined to be optimal for the attractor reconstruction of the response acceleration obtained at all measurement points.

Figure 4 shows the time history and Fourier amplitude of response data observed at the sensor S1. From the Fourier amplitude, results show that several vibration modes are excited because of the chaotic input signal.

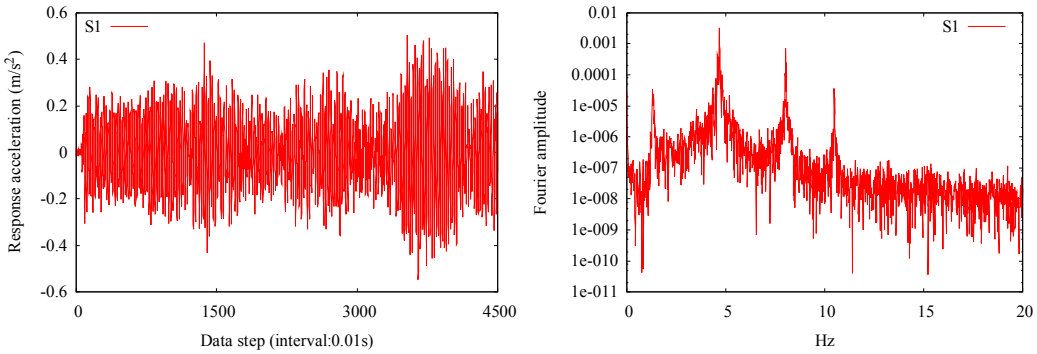

(a) Time history of response . (b) Fourier amplitude of response.

Figure 4. Time history and FFT results of Response

Figure 5 shows the time history and Fourier amplitude of wavelet coefficients corresponding to the first mode vibration. The Fourier amplitude in Fig. 5(b) is observed at Sensor S1. The amplitude of wavelet coefficients observed from the lower story with sensor S1 to the higher story with sensor S7 indicates the linear increase trend, as shown in Fig. 5(a). Also, Figs. 4(b) and 5(b) show that the components of the first mode vibration can be extracted accurately from the response data, although wavelet coefficients are not the actual first mode vibration.

When applying the MPF for the identification of dynamical parameters, the number of merged particles was set to n_m=3 in Eq.(16), and the weights β_k were set as follows:

$$\beta_1 = \frac{3}{4}, \beta_2 = \frac{\sqrt{13}+1}{8}, \beta_3 = -\frac{\sqrt{13}-1}{8} \tag{20}$$

As for the time interval of updating ensemble, we consider 2cases of 5 step interval and 10 step interval.

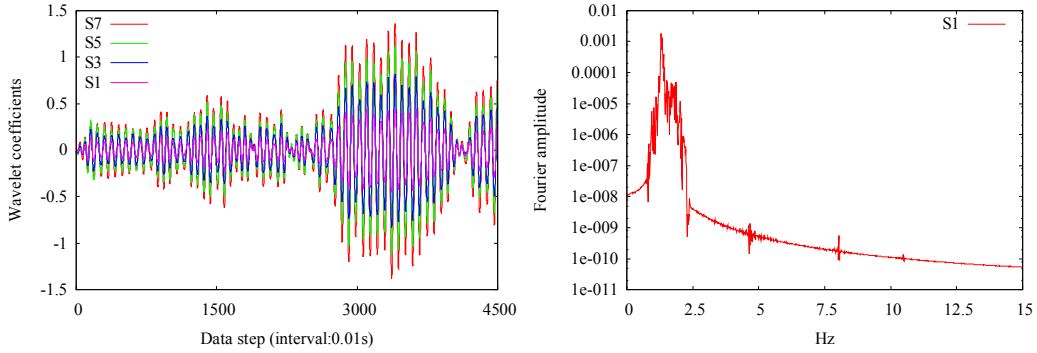

(a) Time history of wavelet coef. (b) Fourier amplitude of wavelet coef.

Figure 5. Time history and FFT results of wavelet coef.

4.1 Results of damage localization by recurrence plots

The result of damage scenario 1, where a column C1 at the first story is replaced with a 30mm-wide column, is depicted in Fig. 6. In this case, a 6.25% reduction in inter-story stiffness occurs at the damage story. Damage Index (*DI*) obtained from the sensors S1 and S2, which are on the damaged story, show larger values among all cases and exhibit about 18% increase. However, at stories immediately after the damage story, *DI* indicates about 1.0 in each and the average amount of the change in *DI* is about 3%. Therefore, the intact stories have not been affected by the damage. From these results, it can be predicted that the first story has something abnormal or that it has damage.

Figure 7 presents results obtained under the situation of damage scenario 2 in which a column at the first story is removed. As portrayed in Fig. 7, the *DI* at the S1 and S2, which are located at the first story, indicates larger values among other sensors. It can be therefore predicted that the first story has something abnormal. Meanwhile, at other stories such as the second, third, and fourth stories, results show that their sensors indicate about 1.0, meaning that their stories remained unchanged before and after damage and that they are intact. It can be predicted from these results that only the first story has damage. Furthermore, also, from the comparison of the results of damage scenario 1 where a column C1 at the first story is replaced with a 30mm-width column, it is considered that *DI* obtained from damage story increases according to the damage magnitude.

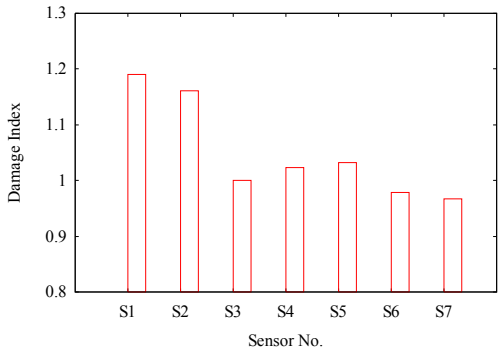

Figure 6. Results for damage scenario 1.

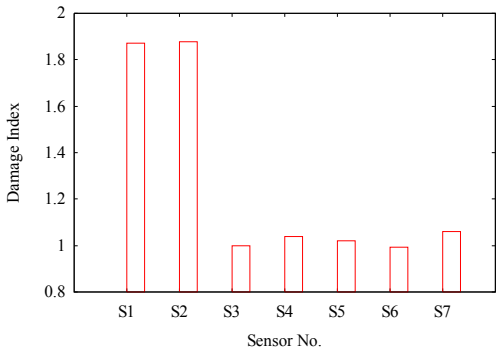

Figure 7. Results for damage scenario 2.

4.2 Results of Damage quantification by merging particle filter

Table 4 shows the results of identification observed by using MPF for damage scenario 1.In this case, ensemble was updated at the 5 step interval. It was found from the results that the

identified structural parameters are close to the real model parameters, especially for the stiffness K and the mass M. However, the stiffness at the 1st story with damage was overestimated, which means that further improvements to identify the structural parameters are needed for a practical tool.

Table 5 shows the identification results for damage scenario 2. In this case, ensemble was updated at the 10 step interval. It was also observed from the results that the identified structural parameters are close to the real model parameters; however, the stiffness at the 1st story with severe damage was also overestimated as well.

The time histories of the identified parameters are shown in Figures 8 and 9. It is found from the figures that each parameter converged at an early stage. This early convergence is considered to be caused by degeneration. The further improvement to avoid this problem is needed as one of future works.

	Mass(kg) True/Estimate, (error)	Stiffness(N/m) True/ Estimate, (error: %)
1st story	2.441/2.309, (-5.42%)	2730.6/2486.9, (-14.61%)
2nd story	2.441/2.256, (-7.59%)	2912.6/2956.0, (1.49%)
3rd story	2.441/2.347, (-3.83%)	2912.6/2860.9, (-1.78%)
4th story	8.353/8.308, (-0.53%)	2912.6/2909.7, (-0.10%)

Table 4. Expected values at final step (scenario 1).

	Mass(kg) True/Estimate, (error: %)	Stiffness(N/m) True/ Estimate, (error: %)
1st story	2.441/2.468, (1.11%)	2184.4／1823.1, (-16.54%)
2nd story	2.441/2.323, (-4.83%)	2912.6／2841.2, (-2.45%)
3rd story	2.441/2.248, (-7.91%)	2912.6／3020.1, (3.69%)
4th story	8.353/8.214, (-1.66%)	2912.6／2969.6, (1.96%)

Table 5. Expected values at final step (scenario 2).

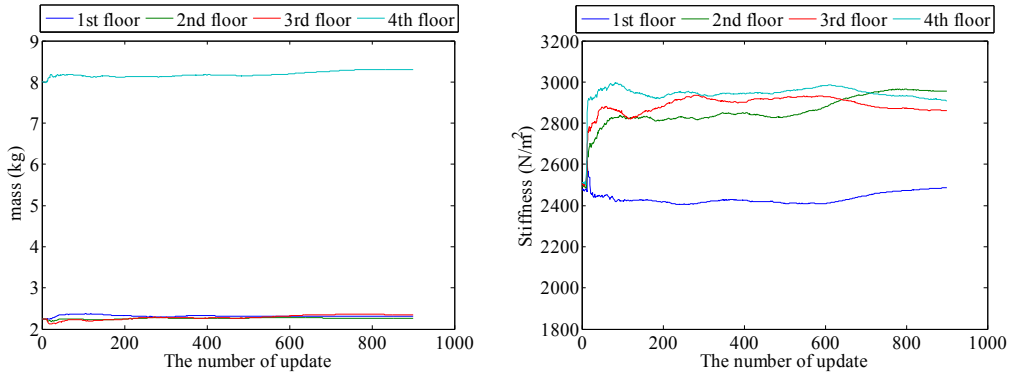

(a) The mass (scenario 1) (b) The stiffness (scenario 1)

Figure 8. Identification results by MPF for damage scenario 1

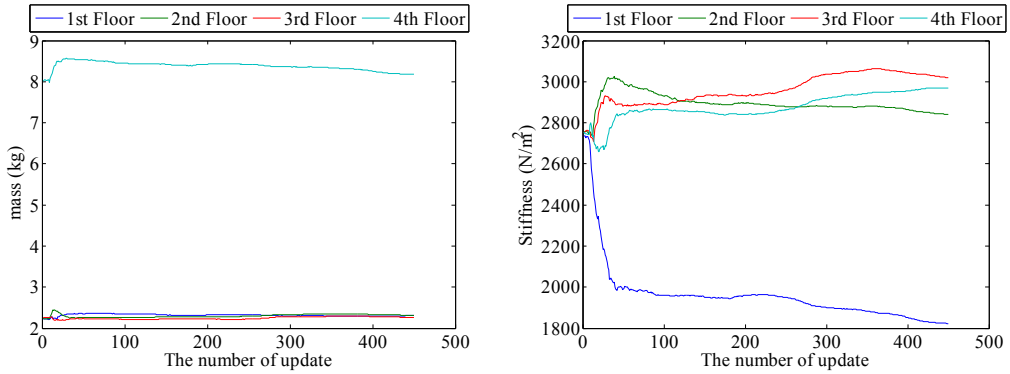

(a) The mass (scenario 1) (b) The stiffness (scenario 1)

Figure 9. Identification results by MPF for damage scenario 1

5 CONCLUSIONS

A first attempt was made in this study to explore an attractor-based health monitoring system using chaotic excitation for damage localization. In evaluation of the reconstructed attractor, recurrence quantification analysis was introduced to detect damage-induced change. In this study, the wavelet coefficient detected from the response data was analyzed to locate the damage, where several threshold values were set to calculate the *%REC*. Laboratory experiments demonstrated that the proposed method can enable detection of the damage location accurately by evaluating the normalized *%REC* of the wavelet coefficient corresponding to the first mode vibration before and after damage.

Second attempt was made to explore merging particle filter for damage quantification. It was found from the experimental results that the identified structural parameters were close to the real model parameters, especially for the stiffness K and the mass M. However, the stiffness at the 1st story with damage was overestimated in both damage scenario cases, which means that further improvements to identify the structural parameters are needed for a practical tool.

REFERENCES

[1] Doebling, S.W., Farrar, C.R. & Prime, M.B. 1998. A summary review of vibration-based identification methods, *Shock and Vibration Digest*, 205(5):631-645.

[2] Farrar, C.R., Duffey, T.A., Doebling, S.W. & Nix. D.A. 1999. “A statistical pattern recognition paradigm for vibration-based structural health monitoring,” in Structural Health Monitoring 2000, pp.764-773.

[3] Bohle, K. & Fritzen., C.P. 2003. Results obtained by minimizing natural frequency and mac-value error of a plate model, *Mechanical Systems and Signal Processing*, 17(1):55-64.

[4] Sohn, H., Farrar, C.R., Hunter, N.F. & Worden, K. 2001. Structural health monitoring using statistical pattern recognition techniques, *Journal of Dynamic Systems, Measurement*, and Control, 123:706-711.

[5] Bodeux, J.B. & Golinval. J.C. 2003. Modal identification and damage detection using the data-driven stochastic sub-space and arma methods, *Mechanical Systems and Signal Processing*, 17(1):83-89.

[6] Worden, K., Manson, G. & Allman, D. 2003. Experimental validation of a structural health monitoring methodology –part I: novelty detection on a laboratory structure, *Journal of Sound and Vibration*, 259(2):323-343.

[7] Okafor, A.C. & Dutta, A. 2000. Structural damage detection in beams by wavelet transforms, *Smart Materials and Structures*, 6:906-917.

[8] Hou, Z., Noori, M. & Amand. R.S. 2000. Wavelet-based approach for structural damage detection, *Journal of Engineering Mechanics*, 126(7):677-683.

[9] Owen, J.S., Eccles, B.J., Choo, B.S. & Woodings. M.A. 2001. The application of auto-regressive time series modeling for the time-frequency analysis of civil engineering structures, *Engineering Structures*, 23:521-536.

[10] Nichols, J.M., Todd, M.D., Seaver, M. & Virgin., L.N. 2003. Use of chaotic excitation and attractor property analysis in structural health monitoring, *Physical Review E*, 67:016207 1-8.

[11] Nichols, J.M., Todd, M.D., Seaver, M., Trickey, S.T., Pecora, L.N. & Moniz. L. 2003. Controlling system dimension: A class of real systems that obey the Kaplan-Yorke conjecture, *Proceedings of the National Academy of Sciences of the United States of America* (PNAS), 100(26):15299-15303.

[12] Nichols, J.M., Trickey, S.T., Seaver, M. 2006. Damage detection using multivariate recurrence quantification analysis, *Mechanical Systems and Signal Processing*, 20:421-437.

[13] Sato, T. and Tanaka, Y. 2010. Minor damage detection using chaotic excitation and recurrence analysis, Proceeding of the international symposium on advances in Urban Safety (SAUS2010), Kobe, Japan, 2010, pp. 141-150.

[14] Eckmann, J.-P., Kamphorst, D. & Ruelle D. 1987. Recurrence plots of dynamic systems, *Europhysics* Letter 4:973-977.

[15] Nakano, S., Ueno G. and Higuchi, T. 2007. Merging particle filter for sequential data assimilation, *Nonlinear Processes in Geophysics*, 14:395-408.

[16] Webber Jr., C.L. & Zbilut, J.P. 1994. Dynamical assessment of Physiological systems and states using recurrence plot strategies, *Journal of Applied Physiology*, 76:965-973.

[17] Gordon, N. J., Salmond, D. J. and Smith, A. F. M. 1993. Novel approach to nonlinear/non-Gaussian Bayesian state estimation, *IEEE Proceedings of Radar Signal Processing*, 140(2): 107-113.

[18] Kitagawa, G. 1996. Monte Carlo Filter and Smoother for Non-Gaussian State Space Models, *Journal of Computational and Graphical Statistics*, 5(1):1-25.